Int. J. Electrochem. Sci., 15 **(2020)** 9294 – 9299, doi: 10.20964/2020.09.28

International Journal of
ELECTROCHEMICAL
SCIENCE
www.electrochemsci.org

Short Communication

$Ce_{1-x}Pr_xO_{2-d}$ (x = 0.1, 0.2, 0.3 and 0.4) as Suspended Catalysts in a Hybrid Direct Carbon Fuel Cell

K. Kammer Hansen[*], *L. Deleebeeck*

Department of Energy Conversion and Storage, Technical University of Denmark, DK-2800, Kgs. Lyngby, Denmark
[*]E-mail: kkha@dtu.dk

Received: 27 April 2020 / *Accepted:* 4 June 2020 / *Published:* 10 August 2020

$Ce_{1-x}Pr_xO_{2-d}$ catalysts (x = 0.1, 0.2, 0.3 and 0.4) (CPOx) are synthesized using the glycine nitrate process. The CPO are used as catalysts in a hybrid direct carbon fuel cell with good results. The highest effect is achieved with the CPO30 compound.

Keywords: HDCFC; CPO; Anode-supported

1. INTRODUCTION

More efficient solutions to convert biomass into electricity are highly wanted. The direct carbon fuel cell offers such a solution. In a direct carbon fuel cell solid fuel carbonaceous (e.g., biomass) can be converted directly into electricity without combustion. There are several types of direct carbon fuel cells. A variant of this is a combination of a molten carbonate fuel cell and a solid oxide fuel cell, a so-called hybrid direct carbon fuel cell (HDCFC), see for example [1]. The HDCFC concept is illustrated in Figure 1, for an anode supported configuration, with a conventional Ni/yttria-stabilized zirconia (YSZ) anode as used in this project.

Fig. 1. Schematic drawing of a hybrid direct carbon fuel cell based on an anode supported cell. The oxidation of carbon is shown to proceed via gasification.

The suggested reaction partway in Figure 1 is via gasification:

(1) $C + CO_2 \rightarrow 2CO$

(2) $CO + O^{2-} \rightarrow CO_2 + 2e^-$

This reaction pathway has a much lower theoretical efficiency than the direct total oxidation of C [1]:

(3) $$C + 2O^{2-} \rightarrow CO_2 + 2e^-$$

This can, in part, be overcome by using a cathode supported cell concept, addressed in earlier works [2, 3]. One additional problem with the HDCFC is a low power output. To partially overcome this suspended catalyst can be added to the carbonate/carbon suspension, see i.e. [4]. In this work $Ce_{1-x}Pr_xO_{2-d}$ catalysts (x = 0.1, 0.2, 0.3 and 0.4) (CPOx) were synthesized and added to the suspension in the anode chamber (carbonate + carbonaceous fuel). CPOx are mixed electronic and ionic conducting oxides which adopt the fluorite structure; Pr can have the oxidation states (III) and (IV). This and doping with Pr-oxide into ceria is descripted in equations (4) and (5) using Kröger-Vink notation.

(4) $$2Ce_{Ce}^{x} \xrightarrow{PrO_{2-\delta}} 2Pr'_{Ce} + V_O^{\cdot\cdot} + ½O_2(g)$$

(5) $$2Pr_{Ce}^{x} + O_O^{x} \leftrightarrows 2Pr'_{Ce} + V_O^{\cdot\cdot} + ½O_2(g)$$

Doping with Pr-oxide increases both the ionic and electronic conductivity of ceria [5, 6]. Ionic conductivity is 0.033 S/cm for CPO40 at 700 °C [7], which is higher than for CeO_2 ($8.2x10^{-4}$ S/cm [8]).

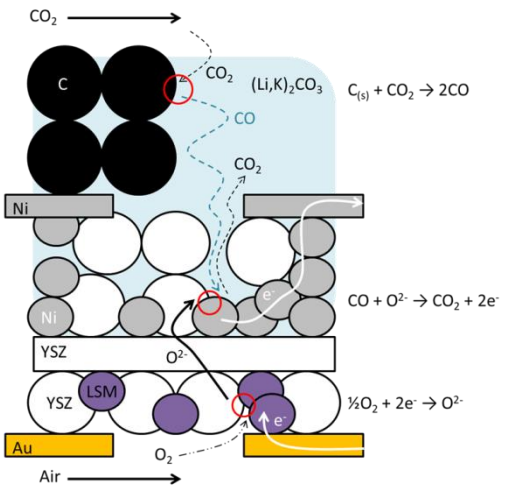

Figure 1. Schematic drawing of a hybrid direct carbon fuel cell based on an anode supported cell. The oxidation of carbon is shown to proceed via gasification.

CeO_2 and CPO20 are catalytically active towards CO oxidation. This is probably due to the co-existence of Pr(III) and Pr(IV) in CPOx, this is in addition to this Ce(III) and Ce(IV) found in doped and undoped ceria-based oxides. The presence of Pr(III)/Pr(IV) and Ce(III)/Ce(IV) reduction/oxidation (redox) couples leads to higher concentrations of surface oxygen vacancy sites, resulting in a higher adsorption/reaction rate of CO (i.e., CPO20 > CeO_2) [9]. Even though CPO can degrade, with resulting formation of PrO_x secondary phases [10], these phases are catalytically active towards CO oxidation

[10]. In addition, a mixture of 5:1 wt% CeO_2:PrO_x has been reported to be a better catalyst for soot oxidation than both CeO_2 and $Ce_{5x}Pr_xO_{2-\delta}$ [11]. Therefore, the formation of secondary phases, like Pr_7O_{12}, which is formed when the oxygen partial pressure (P_{O2}) is low and the temperature are high [12, 13] might not inhibit/alter the catalytic activity of CPO40 in a HDCFC anode.

An anode chamber mixtures of 4:1:1 wt% C black acetylene: (Li-K)$_2CO_3$:CPO40 has previously been reported, at 800 °C and 96-4 vol% N_2-CO_2 anode atmosphere, to give rise to a 987 mV open circuit voltage (OCV), and generation of 45.9 mW/cm^2 at 52 mA/cm^2 in HDCFC [4]. A similarly mixture with bituminous coal instead of carbon black was reported to give rise to a 1148 mV OCV and result in the generation of a maximum power density of 110.8 mW/cm^2 at 800 °C with an anode atmosphere containing 80-20 vol% N_2-CO_2 [14]. In that work several suspended catalysts was tried, among them different manganese oxides, and doped ceria (Sm, Gd and as mentioned CPO40). The best performance was achieved by the Mn(III)-oxide, with a power density of 46.2 mWcm^{-2}. Undoped ceria gave rise to a power density of 42.5 mWcm^{-2} [15]. All at 755 ^{o}C. Alternatives anodes are descripted in [16-18].

2. EXPERIMENTAL

CPOx was synthesized using the glycine-nitrate process accordingly to [19]. The CPO's investigated in this study was the following; CPO10, CPO20, CPO30 and CPO40 (CPOx, $Ce_{1-x}Pr_xO_{2-\delta}$). The powders were all shown to be phase pure accordingly to powder X-ray diffraction (XRD).

The anode chamber was loaded with a mixture with the compostion 4:1:1 wt% carbon black acetylene (C): (62-38 wt% Li-K)$_2CO_3$):CPOx, and was used after ball-milling at low velocity with ZrO_2 for 3 hrs. As a carbon source carbon black acetylene (99.9+ % purity, Alfa Aesar) was used. The eutectic mixture of 62-38 wt% Li_2CO_3-K_2CO_3 (Sigma Aldrich) was shaked for several hours in order to obtain a proper mixing.

An anode-supported half-cell, with a zirconia (YSZ) electrolyte and NiO/zirconia (YSZ) anode was used as received (Topsoe Fuel Cell A/S) and screen-printed with an lanthanum strontium manganite (LSM)-YSZ cathode and sintered at 1050 °C for 2 hrs. In additon to this a LSM cathode current collector was added. The active area is 12 cm^2. Current collector (81-19 wt% Au paste-graphite) was also used on the anode.

Experimental setup is as in [20]. The Inconel cell house [21] was with an anode chamber containing ~ 2 g of the catalyst and the fuel. A gas flow plate was used on the cathode side. After loading in a furnace the cell was loaded with a weight of 8 kg. The cell was heating to 800 °C at 180 °C/hr with flows of 5 L/hr N_2 at the anode and 19 L/hr air at the cathode. A stable OCV at 800 °C was established, this indicates the reduction of the NiO in the anode layer. In the final step, the cell was set to temperature 715 °C. The gasses supplied during test were air (19 L/hr) at the cathode and 96-4 vol% N_2-CO_2 (5 L/hr total flow) at the anode.

Anode and cathode voltages and current are monitored. Recording of the current-voltage (I-V) curves were done by varying between OCV and the current corresponding to maximum power density.

3. RESULTS and DISCUSSION

The results are shown in Figures 2 and 3. The maximum powder density was found for CPO30. All the power densities are higher than that obtained for the uncatalyzed reaction, as reported in [22]. All the I-V curves shows a change in slope at around 700 mV.

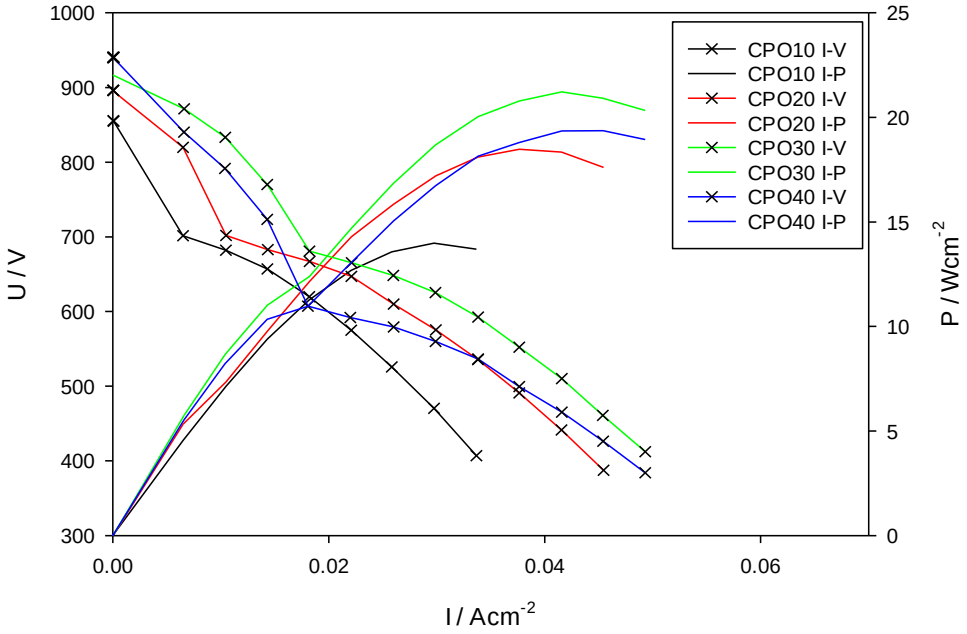

Figure 2. I-V and I-P curves recorded at 715 ^{o}C with different types of CPO's as suspended catalysts. The powder density finds its maximum for CPO30.

The OCV increases with increasing Pr-content, see Figure 3.

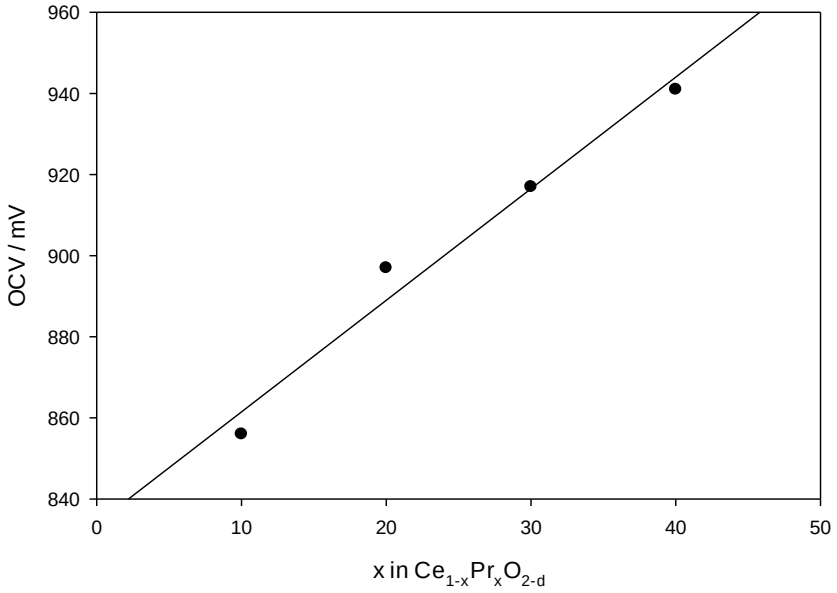

Figure 3. The OCV as a function of Pr content increases with increasing Pr content.

The mechanisms of promotion of anode chamber processes observed upon inclusion of CPOx are likely related to catalysis through the Pr(IV)/Pr(III) redox couple. Additionally, CPOx with higher amounts of Pr are better electronic and ionic conductors than CeO_{2-x}. In this way, CPOx may extent the electrochemically active surface area. The decrease in activity from CPO30 to CPO40 could be related to lower content of Ce(III)/Ce(IV). The CPO40 in this study has a higher activity than shown in [4]. This could be due to better mixing. The Pr-containing cerium oxides performs better than the both the Sm- and Gd-doped cerium oxides, probably due to the Pr(III/IV) redox couple, compared to the fixed oxidation states of Gd(III) and Sm(III) [14]. The enhancement of performance is most likely due to a reaction pathway proceeding through gasification.

The inflection at around 700 mV shown in the I-V curves may be related to the reduction of NiO to Ni. This will lead to constant potential, due to Gibbs phase rule.

The increase in OCV with increasing Pr content could be due to higher gasification of the C due to catalysis by the Pr(III)Pr(IV) redox couple, as.

4. CONCLUSION

CPO's showed a high catalytic activity towards carbon oxidation probably via coal gasification, leading to a relative high performance of the direct carbon fuel cell. Catalytic promotion by CPOx is proposed to be related to the presence of the Pr(IV)/Pr(III) and Ce(IV)/Ce(III) redox couples.

ACKNOWLEDGEMENTS
Ole 'Ørn' Hansen is thanked for performing the experiments.

References

1. L. Deleebeeck, K. Kammer Hansen, *J. Solid State Electrochem*., 18 (2014) 861
2. V. Gil, J. Gurauskis, L. Deleebeeck, E. Stamate, K. Kammer Hansen, *Int. J. Hydrogen Energy*, 42 (2017) 4311
3. K. Kammer Hansen, L. Deleebeeck, V. Gil, in preparation
4. L. Deleebeeck, D. Ippolito, and K. Kammer Hansen, *ECS Trans.*, 61(1) (2014) 225.
5. Y. Takasu, T. Sugino, Y. Matsuda, J. Appl. Electrochem. 14 (1984) 79.
6. P. Fabry, M. Kleitz, *J. Solid State Chem*., 57 (1974) 165.
7. M. J. Chen, S. Cheng, F. Y. Wang, J. F. Lee, and Y. L. Tai, *ECS Trans.,* **7**(1) (2007) 2245
8. H. Inaba and H. Tagawa, *Solid State Ionics,* 83(1-2) 1 (1996) 1
9. L. Gonzalez Rovira, J.J. Degado, K. El Amrani, E. del Rio, X. Chen, J.J. Calvino and F.J. Botana, *Catal. Today*, 180 (2012) 167
10. Y. Borchert, P. Sonstrom, M. Wilhelm, H. Borchert, and M. Baumer, *J. Phys. Chem. C*, 112 (2008) 3054
11. M.A. Malecka, L. Kepinski, and W. Mista, *Appl. Catal. B-Environ.*, 74 (2007) 290
12. B.G. Hyde, D.J.M. Bevan, and L. Eyring, *Phil. Trans. Royal Soc. London A: Math., Phys. Eng. Sci.*, 259 (1966) 583
13. V. Thangadurai, R.A. Huggins, and W. Weppner, *J. Solid St. Electrochem.*, 5 (2001) 531

14. K. Liu, K. Ye, G. Cheng, J. Wang, J. Yin, and D. Cao, *Electrochim. Acta*, 135 (2014) 270
15. J. Liu, J.S. Qiao, H. Yuan, J. Feng, C. Sui, Z.H. Wang, W. Sun, K.N. Sun, Electrochim. Acta 232 (2017) 174
16. K. Sun, J. Liu, J. Feng, H. Yuan, M. He, C. Xu, Z. Wang, W. Sun, J. Qiao, J. Power Sources¸ 365 (2017) 109
17. M. Ma, J. Qiao, X. Yang, C.M. Xu, R.Z. Ren, W. Rongzheng, W. Sun, K.N. Sun, Z.H. Wang, ACS Applied Materials & Interfaces, 12(11) 12938 (2020) 12938
18. H. Xie, S. Zhai, C. Chen, B. Chen, T. Liu, Y. Zhang, Y. Zhang, M. Ni, Z.P. Shao, Z. Shao, Applied Energy, article Number: 260 (2020) 114197
19. L.A. Chick, L.R. Pederson, G.D. Maupin, J.L. Bates, L.E. Thomas, and G.J. Exarhos, *Mater. Lett.*, 10(1-2) (1990) 6
20. A. C. Chien, G. Corre, R. Antunes, and J. T. S. Irvine, *Int. J. Hydrogen Energy*, 38(20) (2013) 8497
21. L. Deleebeeck, D. Ippolito, and K. Kammer Hansen, *J. Electrochem. Soc.*, 162(3) (2015) F327
22. L. Deleebeeck, and K. K. Hansen, *J. Electrochem. Soc*., 161(1) F33 (2014) F33
23. D. Ippolito, L. Deleebeeck, K. Kammer Hansen, *J. Electrochem. Soc*., 164 (2017) F328

© 2020 The Authors. Published by ESG (www.electrochemsci.org). This article is an open access article distributed under the terms and conditions of the Creative Commons Attribution license (http://creativecommons.org/licenses/by/4.0/).